2020 59th IEEE Conference on Decision and Control (CDC)
Jeju Island, Republic of Korea, December 14-18, 2020

Open and closed loop traffic control by connected automated vehicles

Tamás G. Molnár, Devesh Upadhyay, Michael Hopka, Michiel Van Nieuwstadt, and Gábor Orosz

***Abstract*— The problem of controlling traffic using connected automated vehicles is approached by utilizing Lagrangian traffic models. A continuum model with time delay is introduced in the Lagrangian frame in order to capture the open loop dynamics of the traffic behind a vehicle of prescribed motion. The stability of the open loop system is analyzed and compared to that of a benchmark car-following model. Finally, the Lagrangian traffic models are used to propose a longitudinal controller for connected automated vehicles that allows them to respond to connected vehicles behind to stabilize the upstream traffic in a closed loop fashion.**

I. INTRODUCTION

Today's research on vehicle and traffic control is significantly influenced by technologies that establish connectivity between the traffic infrastructure, vehicles and other traffic participants. Vehicles equipped with vehicle-to-everything (V2X) communication devices are able to acquire real time data about other (even distant) traffic participants, which is challenging using on-board sensors. This additional information enables engineers to design and control connected automated vehicles (CAVs) that are able to respond to the upcoming traffic and drive in a safe, stable and efficient manner [1] while mitigating traffic congestions behind via smooth driving [2].

The notion of regulating traffic with the help of vehicles is called Lagrangian traffic control [3], [4], [5], [6], [7], [8]. The term *Lagrangian* refers to the vehicle-based viewpont of traffic as opposed to location-based *Eulerian* approaches. Similarly, the transmitted data that CAVs rely on is often called as Lagrangian data [9], since it typically contains information about certain connected vehicles. The data is often supplemented by traffic flow models that estimate the impact of the CAVs on the traffic behind them (upstream) as well as predict the flow ahead (downstream). Many of the early models were constructed in a location-based Eulerian frame, however, today's applications call for models in vehicle-based Lagrangian frame [10], [11], [12], [13], which are more compatible with the Lagrangian data transmitted by V2X connectivity.

In this paper, we construct a Lagrangian continuum traffic flow model with time delays originating from sensing, communication, feedback, actuation and human reaction time. Delayed continuum models have shown up in the literature recently [14], [15], [16], [17], and now we extend our work on velocity based models [18], [19] to acceleration based ones. An important property of the proposed model is its vehicle-based Lagrangian formulation, which is tailored to applications with connectivity. We analyze the string stability [20] of open loop traffic given by the model. Finally, we propose a Lagrangian traffic controller where the CAV stabilizes the upstream traffic by responding to connected vehicles behind. This leads to the notion of a virtual ring.

T. G. Molnár and G. Orosz are with the Department of Mechanical Engineering and G. Orosz is also with the Department of Civil and Environmental Engineering, University of Michigan, Ann Arbor, MI, USA; molnart@umich.edu, orosz@umich.edu.

D. Upadhyay, M. Hopka and M. Van Nieuwstadt are with the Ford Research and Innovation Center, Dearborn, MI, USA; dupadhya@ford.com, mhopka@ford.com, mvannie1@ford.com.

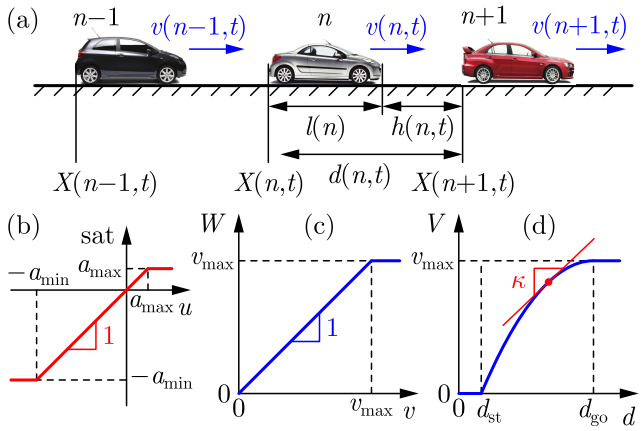

Fig. 1. Illustration of (a) car-following on a single lane, (b) the saturation function (2), (c) the saturation function (4) and (d) the range policy (5).

II. BENCHMARK CAR-FOLLOWING MODEL

As a benchmark to construct continuum models, we consider the car-following model shown by Fig. 1(a), where vehicle n responds to the motion of vehicle $n+1$. We denote the position of vehicle n as a function of time t by $X(n,t)$ and its speed by $v(n,t)$. The headway between the vehicles is $h(n,t)$, which is directly related to the distance $d(n,t) = X(n+1,t) - X(n,t)$ by the length $l(n)$ of vehicle n: $d(n,t) = h(n,t) + l(n)$.

We consider that the acceleration $\partial_t v(n,t)$ of vehicle n is set directly by its control input $u(n,t-\tau)$ according to

$$\begin{aligned} \partial_t X(n,t) &= v(n,t)\,, \\ \partial_t v(n,t) &= \mathrm{sat}(u(n,t-\tau))\,. \end{aligned} \tag{1}$$

The control input is subject to a delay τ, which models the communication and feedback delays in CAVs, the actuation delays, and the reaction time of human drivers. Since the acceleration capability of vehicles is limited, the saturation function sat is applied on the control input u according to

$$\mathrm{sat}(u) = \min(\max(-a_{\min}, u), a_{\max})\,, \tag{2}$$

978-1-7281-7447-1/20/$31.00 ©2020 IEEE

see Fig. 1(b). Here $a_{\min}$ and $a_{\max}$ represent the maximum deceleration and acceleration capability of the vehicles, which may depend on the speed. For simplicity, we assume homogeneous traffic flow where the delay τ, the saturation function sat and the control law governing the input u are identical for all vehicles (independent of n). The model can be extended to heterogeneous traffic flows where any of these features explicitly depends on the vehicle index n.

To define the control input u, we use the optimal velocity model [21], [22]. This model can represent human-driven vehicles (HVs) [23], and it can also be used to build controllers for CAVs [1]. Accordingly, the control input is

$$u(n,t) = \alpha\big(V(X(n+1,t) - X(n,t)) - v(n,t)\big) + \beta\big(W(v(n+1,t)) - v(n,t)\big), \quad (3)$$

where

$$W(v) = \min(v, v_{\max}), \quad (4)$$

$$V(d) = \min(\max(0, F(d)), v_{\max}). \quad (5)$$

The second term in (3) ensures that vehicle n adjusts its speed to the speed of vehicle $n+1$ or to the speed limit $v_{\max}$, whichever is smaller; see the definition of W in (4) and in Fig. 1(c). The first term in (3) controls the distance between vehicles n and $n+1$ by feeding back the difference of the speed $v(n,t)$ from the desired speed V that depends on the distance $d(n,t)$. The desired speed is given by the range policy (5) illustrated in Fig. 1(d). Accordingly, vehicle n shall stop when the distance $d(n,t)$ drops below d_{st}; shall increase its speed according to function $F(d)$ when the distance is above d_{st} but does not exceed d_{go}; and shall travel at the speed limit $v_{\max}$ when the distance is above d_{go}.

III. CONTINUUM MODELS WITH DELAYS

In order to construct continuum models with delays, we use the approach in [18], [19] introduced for velocity based models. We consider the vehicle index n as a continuous variable, and we expand the motion of vehicle n around the motion of vehicle $n+1$ via the Taylor series of $X(n,t)$ with respect to its first argument around $n+1$ up to order M:

$$X(n,t) \approx \mathcal{T}_n^M X(n+1,t), \quad (6)$$

where $\mathcal{T}_n^M$ indicates the operator

$$\mathcal{T}_n^M = \sum_{m=0}^{M} \frac{(-1)^m}{m!} \partial_n^m. \quad (7)$$

The speed $v(n,t)$ and acceleration $\partial_t v(n,t)$ can be expanded the same way via $\mathcal{T}_n^M$. The order M of the expansion determines the order of the resulting continuum model with respect to n, thus we shortly call M as model order.

Substituting the expansion of position, speed and acceleration into (1,3) and shifting index $n+1$ to n leads to

$$\begin{aligned} &\partial_t X(n,t) = v(n,t), \\ &\mathcal{T}_n^M \partial_t v(n,t) = \mathrm{sat}(\hat{u}(n,t-\tau)), \\ &\hat{u}(n,t) = \alpha\left(V\big(X(n,t) - \mathcal{T}_n^M X(n,t)\big) - \mathcal{T}_n^M v(n,t)\right) \\ &\qquad + \beta\left(W(v(n,t)) - \mathcal{T}_n^M v(n,t)\right). \end{aligned} \quad (8)$$

For example, the simplest case $M = 1$ yields

$$\begin{aligned} &\partial_t X(n,t) = v(n,t), \\ &\partial_t v(n,t) - \partial_{tn} v(n,t) = \mathrm{sat}(\hat{u}(n,t-\tau)), \\ &\hat{u}(n,t) = \alpha\big(V(\partial_n X(n,t)) - v(n,t) + \partial_n v(n,t)\big) \\ &\qquad + \beta\big(W(v(n,t)) - v(n,t) + \partial_n v(n,t)\big), \end{aligned} \quad (9)$$

cf. (1,3). Note that the limit $M \to \infty$ recovers the car-following model (1,3).

The constructed model (8) is a Lagrangian model, since it is formulated in terms of the vehicle index n and time t. The model can be converted to the Eulerian frame that uses the location x along the highway and time t as independent variables. In Eulerian frame, the traffic density $\rho(x,t)$ and speed $\nu(x,t)$ can be chosen as dependent variables, which satisfy the following relationships [13]: $\partial_t X(n,t) = v(n,t) = \nu(X(n,t),t)$ and $\partial_n X(n,t) = 1/\rho(X(n,t),t)$.

As an example, we transform (9) to the Eulerian frame by substituting the above relationships between X, v and ν, ρ. Carrying out differentiations according to the chain rule and substituting $X(n,t) \mapsto x$ finally leads to the Eulerian counterpart of the continuum model (9) in the form

$$\begin{aligned} &\partial_t \rho(x,t) + \partial_x(\rho(x,t)\nu(x,t)) = 0, \\ &\partial_t \eta(x,t) + \nu(x,t)\partial_x \eta(x,t) = \mathrm{sat}(\mu(x-\xi, t-\tau)), \\ &\mu(x,t) = \alpha\big(V(\rho^{-1}(x,t)) - \eta(x,t)\big) \\ &\qquad + \beta\big(W(\nu(x,t)) - \eta(x,t)\big), \\ &\eta(x,t) = \nu(x,t) - \partial_x \nu(x,t)\rho^{-1}(x,t). \end{aligned} \quad (10)$$

Here, the first equation describes the conservation of the number of vehicles on the highway, which can be derived from the identity $\partial_{tn} X(n,t) = \partial_{nt} X(n,t)$. The second equation involves the spatial delay ξ, which indicates the distance that vehicle n travels during the delay period, i.e., $\xi = X(n,t) - X(n,t-\tau)$. This parameter is related to the Eulerian traffic measures implicitly by

$$\int_{t-\tau}^{t} \rho(x,\tilde{t})\nu(x,\tilde{t})\mathrm{d}\tilde{t} = \int_{x-\xi}^{x} \rho(\tilde{x}, t-\tau)\mathrm{d}\tilde{x}; \quad (11)$$

see [18], [19] for explanation.

Note that (10) reduces to a form similar to the Aw-Rascle-Zhang (ARZ) model [24], [25] in the special case where sat is omitted, $\tau = 0$, $\xi = 0$ and $\beta = 0$. The difference from the ARZ model is that $-\partial_x \nu/\rho$ shows up in η in (10) instead of a pressure term $p(\rho)$ and $-\alpha\eta$ is present on the right-hand side instead of $-\alpha\nu$.

Continuum models with $M > 1$ can be expressed in the Eulerian frame similarly to (10). However, further on we refrain from using the Eulerian frame due to the increased complexity caused by the state-dependent spatial delay ξ.

IV. OPEN LOOP STABILITY

One of the most important aspects of traffic control is the mitigation of traffic congestions on highways. The onset of congestion waves is directly related to the string stability of traffic, which tells us whether perturbations (such as

velocity fluctuations) are attenuated upstream along a chain of vehicles. In what follows, we analyze the string stability of the introduced traffic flow models that represents the open loop traffic dynamics. Ensuring stability will be the objective of Sec. V, where a closed control loop will be introduced.

The literature contains various definitions of string stability [20]. We consider linear input-to-output stability with respect to $\mathcal{L}_2$ norm, as given by the string stability definition below. We analyze the string stability of the uniform flow

$$v(n,t) \equiv v^*\,, \quad X(n,t) = v^* t + n d^* + X(0,0) \tag{12}$$

of constant speed v^* and spacing d^*.

We consider speed perturbations $\tilde{v}(n,t)$ around the uniform flow in the form $v(n,t) = v^* + \tilde{v}(n,t)$. We determine whether these perturbations amplify or decay along a chain of vehicles, that is, we investigate stability with respect to the vehicle index n by following [18], [19]. We achieve this by linearizing models (1,3) and (8) around the uniform flow (12) and considering velocity fluctuations in the form

$$\tilde{v}(n,t) = v_{\mathrm{amp}} \mathrm{e}^{st} \mathrm{e}^{-\lambda(s)n}\,. \tag{13}$$

Note that $\exp(\lambda(s))$ is the transfer function between the velocity fluctuations $\tilde{v}(n+1,t)$ and $\tilde{v}(n,t)$.

For $s = \mathrm{i}\omega$, $\omega > 0$ the velocity fluctuations are harmonic in time with angular frequency ω. The fluctuations decay upstream (as $n \to -\infty$) provided that

$$\left|\mathrm{e}^{\lambda(\mathrm{i}\omega)}\right| < 1\,, \quad \forall \omega > 0 \tag{14}$$

or, equivalently,

$$\Re(\lambda(\mathrm{i}\omega)) < 0\,, \quad \forall \omega > 0\,, \tag{15}$$

which we use as string stability condition [18], [19]. The real part $\Re(\lambda(\mathrm{i}\omega))$ of the exponent $\lambda(\mathrm{i}\omega)$ determines whether velocity fluctuations amplify or decay upstream. The imaginary part $\Im(\lambda(\mathrm{i}\omega))$, also called as the wave number, gives the frequency of perturbations in space (with respect to n), and the direction of their propagation: waves where $\Im(\lambda(\mathrm{i}\omega))$ is negative (positive) propagate upstream (downstream). During the physical interpretation of the models, integer vehicle indices shall be considered only. Thus, velocity perturbations of period less than 2 in terms of the vehicle index n, i.e., wave number larger than π shall be disregarded. Therefore, (14,15) shall be considered subject to $\Im(\lambda(\mathrm{i}\omega)) \in [-\pi, \pi]$.

In what follows, we find the string stable domains in the plane of parameters β and α and visualize them in the form of stability charts. We use the string stability condition (14) when dealing with the car-following model (1,3), while we consider condition (15) for the continuum model (8). These conditions can be transformed to the form

$$P(\omega) > 0\,, \quad \forall \omega > 0\,, \tag{16}$$

where a proper choice of $P(\omega)$ makes the resulting formulas simple. When using $\exp(\lambda(\mathrm{i}\omega))$, we define $P(\omega)$ as

$$P(\omega) = \frac{1}{\omega^2}\left(\mathrm{D}\left(\left|\mathrm{e}^{\lambda(\mathrm{i}\omega)}\right|^2\right) - \mathrm{N}\left(\left|\mathrm{e}^{\lambda(\mathrm{i}\omega)}\right|^2\right)\right), \tag{17}$$

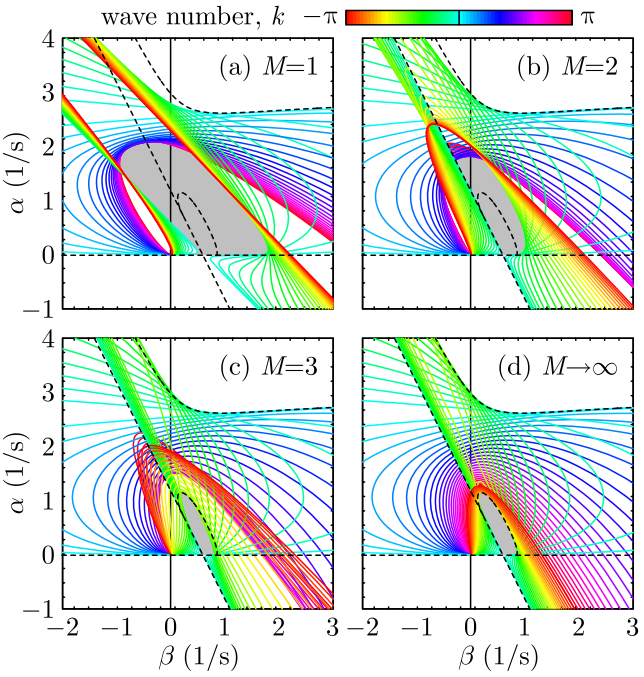

Fig. 2. String stability charts of (a) the continuum model (8) with $M = 1$, (b) $M = 2$, (c) $M = 3$, and (d) the car-following model (1,3) for $\kappa = 0.6\,\mathrm{s}^{-1}$, $\tau = 0.6\,\mathrm{s}$. The stable region is shaded by gray while the string stability boundaries of the car-following model are dashed black.

whereas for the cases utilizing $\Re(\lambda(\mathrm{i}\omega))$, we define

$$P(\omega) = -\frac{1}{\omega^2}\mathrm{N}\big(\Re(\lambda(\mathrm{i}\omega))\big)\overline{\mathrm{D}\big(\Re(\lambda(\mathrm{i}\omega))\big)}\,, \tag{18}$$

where D and N stand for denominator and numerator, respectively, and over-bar denotes complex conjugate.

The boundaries of string stability are found by

$$P(\omega) = 0\,, \qquad \frac{\partial P}{\partial \omega}(\omega) = 0\,, \tag{19}$$

which define a curve parameterized by ω in the (β, α) plane. For $\omega = 0$, the second part of (19) reduces to an identity and the first part defines the stability boundary. Alternatively, the boundaries can also be found by using the ansatz

$$\tilde{v}(n,t) = v_{\mathrm{amp}} \mathrm{e}^{\mathrm{i}\omega t} \mathrm{e}^{-\mathrm{i}kn} \tag{20}$$

with $\omega > 0$, $k \in [-\pi, \pi]$. This leads to a family of curves in the (β, α) plane parameterized by ω and k whose envelope is given by (19).

A. Stability of the Benchmark Car-Following Model

First, we revisit the string stability analysis of the car-following model (1,3), which can also be found in [26]. We consider (1,3) within the saturation limits by dropping sat and W. We linearize the model around the uniform flow (12) and differentiate it with respect to time, which leads to

$$\begin{aligned}\partial_{tt}\tilde{v}(n,t) = \alpha\big(\kappa(\tilde{v}(n+1,t-\tau) - \tilde{v}(n,t-\tau)) - \partial_t \tilde{v}(n,t-\tau)\big) \\ + \beta\big(\partial_t \tilde{v}(n+1,t-\tau) - \partial_t \tilde{v}(n,t-\tau)\big),\end{aligned} \tag{21}$$

where $\kappa = V'(d^*)$ is the slope of the range policy at d^* satisfying $v^* = V(d^*)$; see the illustration in Fig. 1(d).

Substituting (13) into (21) gives the characteristic equation

$$s^2 \mathrm{e}^{s\tau} \mathrm{e}^{\lambda(s)} = \alpha\big(\kappa\big(1-\mathrm{e}^{\lambda(s)}\big) - s\mathrm{e}^{\lambda(s)}\big) + \beta s\big(1-\mathrm{e}^{\lambda(s)}\big). \quad (22)$$

This can be rearranged to $\exp(\lambda(s))$ to find the transfer function of the system in the form

$$\mathrm{e}^{\lambda(s)} = \frac{\beta s + \alpha\kappa}{s^2\mathrm{e}^{s\tau} + (\alpha+\beta)s + \alpha\kappa}\,, \quad (23)$$

whereas $P(\omega)$ in (17) becomes

$$P(\omega) = \omega^2 + \alpha(\alpha+2\beta) - 2(\alpha+\beta)\omega\sin(\omega\tau) - 2\alpha\kappa\cos(\omega\tau)\,. \quad (24)$$

Equations (19,24) define the stability boundaries in the (β,α) plane (see [26] for details), which are depicted by dashed lines in Fig. 2(d) for $\kappa = 0.6\,\mathrm{s}^{-1}$ and $\tau = 0.6\,\mathrm{s}$. The string stable region, where (16) holds, is shaded by gray.

One can also find these boundaries by substituting ansatz (20) into system (21) or, equivalently, substituting $s = \mathrm{i}\omega$, $\lambda(s) = \mathrm{i}k$ into the characteristic equation (22). Then, decomposition into real and imaginary parts leads to

$$\begin{aligned} -\omega^2\cos(\omega\tau + k) &= \alpha\kappa(1-\cos k) + (\alpha+\beta)\omega\sin k\,,\\ -\omega^2\sin(\omega\tau + k) &= -\alpha\kappa\sin k - (\alpha+\beta)\omega\cos k + \beta\omega\,. \end{aligned} \quad (25)$$

Equation (25) can be solved for α and β in the form

$$\begin{aligned} \alpha &= \frac{\omega^2\sin\left(\omega\tau + \frac{k}{2}\right)}{2\kappa\sin\left(\frac{k}{2}\right) + \omega\cos\left(\frac{k}{2}\right)}\,,\\ \beta &= -\frac{\omega\cos\left(\omega\tau + \frac{k}{2}\right)}{2\sin\left(\frac{k}{2}\right)} - \frac{\alpha}{2}\,. \end{aligned} \quad (26)$$

This defines a family curves in the (β,α) plane, which are plotted by colored lines in Fig. 2(d) for various values of k. The envelope of these curves is exactly given by (19,24), since eliminating k from (25) leads to $P(\omega) = 0$.

B. Stability of the Continuum Model

Now we derive the string stability limits of the continuum model (8). We drop sat and W, linearize (8) around (12), and differentiate it with respect to time, which gives

$$\begin{aligned} &\mathcal{T}_n^M \partial_{tt}\tilde{v}(n,t)\\ &= \alpha\left(\kappa\left(\tilde{v}(n,t-\tau) - \mathcal{T}_n^M\tilde{v}(n,t-\tau)\right) - \mathcal{T}_n^M\partial_t\tilde{v}(n,t-\tau)\right)\\ &\quad + \beta\left(\partial_t\tilde{v}(n,t-\tau) - \mathcal{T}_n^M\partial_t\tilde{v}(n,t-\tau)\right). \end{aligned} \quad (27)$$

Substituting (13) into (27) leads to

$$\sum_{m=0}^{M}\frac{\lambda(s)^m}{m!} = \frac{\beta s + \alpha\kappa}{s^2\mathrm{e}^{s\tau} + (\alpha+\beta)s + \alpha\kappa}\,, \quad (28)$$

cf. (23).

If the order M is low, the exponent $\lambda(s)$ can be expressed from (28) in closed form. For $M = 1$, the linearized system (27) reduces to

$$\begin{aligned} &\partial_{tt}\tilde{v}(n,t) - \partial_{ttn}\tilde{v}(n,t)\\ &= \alpha\big(\kappa\partial_n\tilde{v}(n,t-\tau) - \partial_t\tilde{v}(n,t-\tau) + \partial_{tn}\tilde{v}(n,t-\tau)\big)\\ &\quad + \beta\partial_{tn}\tilde{v}(n,t-\tau)\,, \end{aligned} \quad (29)$$

cf. (21), and the solution of the characteristic equation is

$$\lambda(s) = \frac{-s^2\mathrm{e}^{s\tau} - \alpha s}{s^2\mathrm{e}^{s\tau} + (\alpha+\beta)s + \alpha\kappa}\,. \quad (30)$$

Then, string stability can be analyzed by the help of $P(\omega)$ in (18), which reads

$$P(\omega) = \omega^2 + \alpha(\alpha+\beta) - (2\alpha+\beta)\omega\sin(\omega\tau) - \alpha\kappa\cos(\omega\tau)\,. \quad (31)$$

Note that the expression of $P(\omega)$ is similar to the one that was obtained for the car-following model in (24), but now β and κ are replaced by $\beta/2$ and $\kappa/2$. Thus, the string stable domain of the continuum model (8), shown in Fig. 2(a), looks similar to that of the car-following model (1,3), cf. Fig. 2(d). This justifies that the construction (8) of continuum models behaves well from string stability point of view.

When the model order M is larger, $\lambda(s)$ cannot be expressed from (28) in a simple form. In such cases, one can substitute ansatz (20) into (27) and separate the resulting equation into real and imaginary parts. This yields

$$\begin{aligned} -\omega^2\big(\cos(\omega\tau)B - \sin(\omega\tau)A\big) &= \alpha\kappa(1-B) + (\alpha+\beta)\omega A\,,\\ -\omega^2\big(\cos(\omega\tau)A + \sin(\omega\tau)B\big) &= -\alpha\kappa A - (\alpha+\beta)\omega B + \beta\omega\,, \end{aligned} \quad (32)$$

where B and A are the real and imaginary parts of the Taylor expansion of $\exp(\mathrm{i}k)$ up to order M:

$$B = \sum_{l=0}^{\lfloor\frac{M}{2}\rfloor}\frac{(-1)^l k^{2l}}{(2l)!}\,, \quad A = \sum_{l=1}^{\lfloor\frac{M+1}{2}\rfloor}\frac{(-1)^{l-1}k^{2l-1}}{(2l-1)!}\,. \quad (33)$$

Then, (32) can be solved for α and β in the form

$$\begin{aligned} \alpha &= \frac{\omega^2\cos(\omega\tau)(A^2+B^2-B) + \omega^2\sin(\omega\tau)A}{\kappa(A^2+(1-B)^2) + \omega A}\,,\\ \beta &= \frac{-\omega\cos(\omega\tau)A + (\omega\sin(\omega\tau) - \alpha)(A^2+B^2-B)}{A^2+(1-B)^2}\,. \end{aligned} \quad (34)$$

The family of curves defined by (34) is depicted in the (β,α) plane in Fig. 2(a,b,c) for orders $M = 1,\ 2,\ 3$, respectively.

Note that as $M \to \infty$, the coefficients B and A converge to $B \to \cos k$ and $A \to \sin k$, while (34) reduces to (26). This proves the convergence of the string stability boundaries of the continuum model to that of the car-following model. Meanwhile, selecting a low model order M (such as $M = 3$) already gives results close to $M \to \infty$, thus the model complexity does not need to be increased further and potential issues with non-uniform convergence can be avoided.

V. CLOSED LOOP TRAFFIC CONTROL

Finally, based on the proposed Lagrangian model we discuss Lagrangian traffic control, where congestions are mitigated behind a CAV. Assume the scenario in Fig. 3(a) where a CAV indicated by index 0 is the lead vehicle of a traffic flow consisting of HVs. Remark that the motion $X(0,t)$, $v(0,t)$ of the CAV actually imposes boundary conditions for the upstream traffic ($n < 0$), which allows the CAV to control the upstream traffic in a Lagrangian fashion.

If the CAV controls its motion without responding to the vehicles behind, that implies open loop traffic control, which

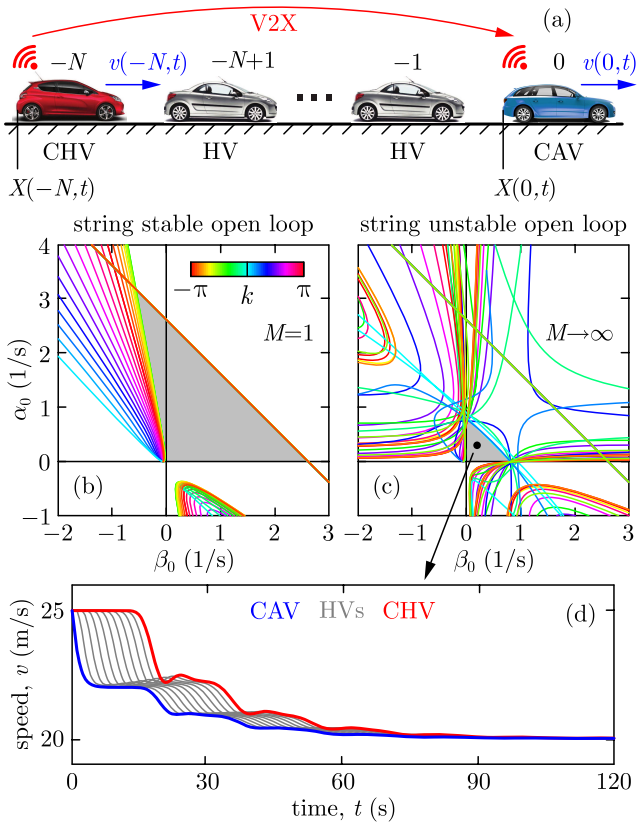

Fig. 3. (a) Illustration of the virtual ring for Lagrangian traffic control by CAVs. (b,c) String stability charts of the closed loop system, where the CAV is described by (35,36), while the upstream traffic is governed by (b) the continuum model (8) with $M = 1$ and (c) the car-following model (1,3). The parameters are $N = 10$, $\sigma = 0.6\,\mathrm{s}$, $\kappa = 0.6\,\mathrm{s}^{-1}$, $\tau = 0.8\,\mathrm{s}$, $\alpha = 0.1\,\mathrm{s}^{-1}$ and $\beta = 0.6\,\mathrm{s}^{-1}$. Gray shading denotes the stable region. (d) Simulation results for the virtual ring consisting of $N = 10$ vehicles behind a CAV. The human driver parameters are the ones identified in [23], i.e., $\tau = 0.8\,\mathrm{s}$, $\alpha = 0.1\,\mathrm{s}^{-1}$ and $\beta = 0.6\,\mathrm{s}^{-1}$, while the range policy V is piecewise quadratic with $F(d) = v_{\max}(1 - (d - d_{\mathrm{st}})^2/(d_{\mathrm{go}} - d_{\mathrm{st}})^2)$ and $d_{\mathrm{st}} = 10\,\mathrm{m}$, $d_{\mathrm{go}} = 60\,\mathrm{m}$, $v_{\max} = 30\,\mathrm{m/s}$. The parameters of the CAV's controller are $\sigma = 0.6\,\mathrm{s}$, $\alpha_0 = 0.3\,\mathrm{s}^{-1}$ and $\beta_0 = 0.2\,\mathrm{s}^{-1}$. Acceleration constraints are given by $a_{\min} = 7\,\mathrm{m/s}^2$ and $a_{\max} = 3\,\mathrm{m/s}^2$.

is described by the models (1,3) and (8) discussed above. However, if one of the HVs behind the CAV (indicated by index $-N$) is a connected human-driven vehicle (CHV), that allows the CAV to respond and close the control loop. This creates a virtual ring of vehicles [23]. In ring configuration, the traffic flow can potentially be stabilized by a single CAV [2]. Below we propose a controller for the CAV and derive the stability conditions of the virtual ring based on the method presented in Sec. IV.

Similarly to (1), the dynamics of the CAV is described by

$$\begin{aligned} \partial_t X(0,t) &= v(0,t)\,, \\ \partial_t v(0,t) &= \mathrm{sat}(u(0,t-\sigma))\,, \end{aligned} \tag{35}$$

where σ is the delay in the control input $u(0,t)$ of the CAV. Following [23], [26], we propose the CAV's controller analogously to (3) in the form

$$u(0,t) = \alpha_0\big(v_{\mathrm{r}}(t) - v(0,t)\big) + \beta_0(W(v(-N,t)) - v(0,t))\,, \tag{36}$$

where α_0 and β_0 are the control gains of the CAV, and v_{r} is a reference speed, potentially dictated by the traffic ahead of the CAV. The dynamics of the virtual ring are defined by (35,36) that describe the CAV's motion ($n = 0$) and by (1,3) or (8) that describe the upstream flow ($n \in [-N, 0)$).

If the reference speed is constant $v_{\mathrm{r}}(t) \equiv v^*$, then the uniform flow (12) exists and satisfies $v^* = V(d^*)$. Below we design α_0 and β_0 such that the uniform flow of the closed loop system is stable and perturbations around the uniform flow are attenuated. To analyze stability, we linearize (35,36) and consider small fluctuations $\tilde{v}_{\mathrm{r}}(t)$ in the reference speed:

$$\begin{aligned} \partial_t \tilde{v}(0,t) = \alpha_0\big(\tilde{v}_{\mathrm{r}}(t-\sigma) - \tilde{v}(0,t-\sigma)\big) \\ + \beta_0\big(\tilde{v}(-N,t-\sigma) - \tilde{v}(0,t-\sigma)\big), \end{aligned} \tag{37}$$

cf. (21). Equation (37) defines the linear dynamics for $n = 0$ while (21) or (27) are the linear models for $n \in [-N, 0)$.

To analyze string stability, we assume the reference speed and the response of the CHV in exponential form

$$\tilde{v}_{\mathrm{r}}(t) = v_{\mathrm{amp,r}} \mathrm{e}^{st}\,, \quad \tilde{v}(-N,t) = v_{\mathrm{amp,r}} \mathrm{e}^{st} \mathrm{e}^{\Lambda(s)}\,, \tag{38}$$

and we also use the exponential solution (13) for the traffic flow between the CAV and the CHV. Substituting (13) and (38) into (37) gives the transfer function of the virtual ring from $\tilde{v}_{\mathrm{r}}(t)$ to $\tilde{v}(-N,t)$ in the form

$$\mathrm{e}^{\Lambda(s)} = \frac{\alpha_0 \mathrm{e}^{\lambda(s)N}}{s\mathrm{e}^{s\sigma} + \alpha_0 + \beta_0 - \beta_0 \mathrm{e}^{\lambda(s)N}}\,. \tag{39}$$

Here, the transfer function $\exp(\lambda(s)N)$ associated with the human-driven traffic can be obtained from (23) for the car-following model (1,3) or by expressing $\lambda(s)$ from (28) for the continuum model (8). For further results on the transfer functions of ring configurations, see [27].

Analogously to Sec. IV, we substitute $s = \mathrm{i}\omega$ ($\omega > 0$) and $\Lambda = \mathrm{i}k$ ($k \in [-\pi, \pi]$) to find the string stability boundaries. Separation into real and imaginary parts leads to

$$\begin{aligned} \omega \sin(\omega\sigma + k) &= \alpha_0(\cos k - R) + \beta_0((1-R)\cos k + S \sin k)\,, \\ \omega \cos(\omega\sigma + k) &= \alpha_0(S - \sin k) + \beta_0(S \cos k - (1-R)\sin k)\,, \end{aligned} \tag{40}$$

where R and S are the real and imaginary parts of $\exp(\lambda(\mathrm{i}\omega)N)$, respectively. Equation (40) can be solved for α_0 and β_0 in the form

$$\begin{aligned} \alpha_0 &= \frac{\omega((1-R)\cos(\omega\sigma) - S\sin(\omega\sigma))}{(S^2 + R^2 - R)\sin k + S\cos k - S}\,, \\ \beta_0 &= \frac{\omega(R\cos(\omega\sigma + k) + S\sin(\omega\sigma + k) - \cos(\omega\sigma))}{(S^2 + R^2 - R)\sin k + S\cos k - S}\,. \end{aligned} \tag{41}$$

The family of curves defined by (41) is shown in the (β_0, α_0) plane for $N = 10$ in Fig. 3(b,c) for the continuum model with $M = 1$ and for the car-following model ($M \to \infty$), respectively. If the human driver parameters α, β, κ and τ define a string stable open loop upstream traffic flow (related to the stable region in Fig. 2), then the string stable region is large for the virtual ring. This is the case for the low-order continuum model in Fig. 3(b). However, if the open loop upstream flow is string unstable, which is the

case for the car-following model in Fig. 3(c), then the string stable region is much smaller. Still, for a finite N one may find a stable (β_0, α_0) parameter combination for the CAV.

To demonstrate the CAV's ability of stabilizing upstream traffic, we selected a stable parameter combination (denoted by black dot in Fig. 3(c)) and performed numerical simulations. We assumed that initially ($t \leq 0$) the vehicles are traveling at $25\,\mathrm{m/s}$ in uniform flow, and then the reference speed changes to constant $20\,\mathrm{m/s}$ ($t > 0$). Fig. 3(d) shows that the CAV is able to gradually slow down to the reference speed without causing traffic congestions behind it. This way, the CAV is able to stabilize the flow of $N = 10$ vehicles. This shows the potential of Lagrangian traffic control to stabilize traffic by CAVs using the concept of a virtual ring.

VI. CONCLUSIONS

In this paper, we have established an approach to construct continuum traffic models from a benchmark car-following model that respect the acceleration capabilities of vehicles while incorporating time delay. Since the proposed model is formulated in vehicle-based Lagrangian frame, it can be used directly in applications with connected automated vehicles (CAVs) where trajectory data from connectivity needs to be used. We have demonstrated that this model recovers the string stability properties of the car following model as its order is increased. Finally, we have discussed how upstream traffic can be stabilized by CAVs by creating a closed control loop in a virtual ring scenario. The control parameters can be designed based on the proposed Lagrangian traffic models. As a future work, we will consider boundary control techniques [28], [29] to synthesize controllers in the virtual ring setup based on Lagrangian continuum traffic flow models.

VII. ACKNOWLEDGMENTS

This project was funded by Ford Motor Co.

REFERENCES

[1] J. I. Ge, S. S. Avedisov, C. R. He, W. B. Qin, M. Sadeghpour, and G. Orosz, "Experimental validation of connected automated vehicle design among human-driven vehicles," *Transportation Research Part C*, vol. 91, pp. 335–352, 2018.

[2] R. E. Stern, S. Cui, M. L. Delle Monache, R. Bhadani, M. Bunting, M. Churchill, N. Hamilton, R. Haulcy, H. Pohlmann, F. Wu, B. Piccoli, B. Seibold, J. Sprinkle, and D. B. Work, "Dissipation of stop-and-go waves via control of autonomous vehicles: Field experiments," *Transportation Research Part C*, vol. 89, pp. 205–221, 2018.

[3] C. Wu, A. Kreidieh, K. Parvate, E. Vinitsky, and A. M. Bayen, "Flow: Architecture and benchmarking for reinforcement learning in traffic control," *arXiv preprint*, no. arXiv:1710.05465, 2017.

[4] M. Čičić and K. H. Johansson, "Traffic regulation via individually controlled automated vehicles: a cell transmission model approach," in *Proceedings of the 21st International Conference on Intelligent Transportation Systems*, Maui, HI, USA, 2018, pp. 766–771.

[5] Y. Zheng, J. Wang, and K. Li, "Smoothing traffic flow via control of autonomous vehicles," *arXiv preprint*, no. arXiv:1812.09544, 2018.

[6] H. Yu, S. Koga, and M. Krstic, "Stabilization of traffic flow with a leading autonomous vehicle," in *Proceedings of the ASME Dynamic Systems and Control Conference*, no. DSCC2018–9239, Atlanta, GA, USA, 2018.

[7] M. L. Delle Monache, J. Sprinkle, R. Vasudevan, and D. Work, "Autonomous vehicles: From vehicular control to traffic control," in *Proceedings of the 58th IEEE Conference on Decision and Control*, Nice, France, 2019, pp. 4680–4696.

[8] N. Bekiaris-Liberis and A. I. Delis, "PDE-based feedback control of freeway traffic flow via time-gap manipulation of ACC-equipped vehicles," *IEEE Transactions on Control Systems Technology*, pp. 1–9, 2020, published online.

[9] J. C. Herrera, D. B. Work, R. Herring, X. Ban, Q. Jacobson, and A. M. Bayen, "Evaluation of traffic data obtained via GPS-enabled mobile phones: The Mobile Century field experiment," *Transportation Research Part C*, vol. 18, no. 4, pp. 568–583, 2010.

[10] G. F. Newell, "A simplified car-following theory: a lower order model," *Transportation Research Part B: Methodological*, vol. 36, no. 3, pp. 195–205, 2002.

[11] L. Leclercq, J. Laval, and E. Chevallier, "The Lagrangian coordinates and what it means for first order traffic flow models," in *Proceedings of the 17th International Symposium on Transportation and Traffic Theory*, 2007, pp. 735–753.

[12] L. Leclercq and J. Laval, "A multiclass car-following rule based on the LWR model," in *Traffic and Granular Flow '07 Part I*. Springer, 2009, pp. 151–160.

[13] J. A. Laval and L. Leclercq, "The Hamilton-Jacobi partial differential equation and the three representations of traffic flow," *Transportation Research Part B: Methodological*, vol. 52, pp. 17–30, 2013.

[14] D. Ngoduy, "Generalized macroscopic traffic model with time delay," *Nonlinear Dynamics*, vol. 77, no. 1–2, pp. 289–296, 2014.

[15] M. Burger, S. Göttlich, and T. Jung, "Derivation of a first order traffic flow model of Lighthill-Whitham-Richards type," in *Proceedings of the 15th IFAC Symposium on Control in Transportation Systems*, vol. 51, no. 9, 2018, pp. 49–54.

[16] A. Tordeux, G. Costeseque, M. Herty, and A. Seyfried, "From traffic and pedestrian follow-the-leader models with reaction time to first order convection-diffusion flow models," *SIAM Journal on Applied Mathematics*, vol. 78, no. 1, pp. 63–79, 2018.

[17] M. Burger, S. Göttlich, and T. Jung, "Derivation of second order traffic flow models with time delays," *Networks & Heterogeneous Media*, vol. 14, no. 2, pp. 265–288, 2019.

[18] T. G. Molnár, D. Upadhyay, M. Hopka, M. Van Nieuwstadt, and G. Orosz, "Lagrangian models for controlling large-scale heterogeneous traffic," in *Proceedings of the 58th IEEE Conference on Decision and Control*, Nice, France, 2019, pp. 3152–3157.

[19] T. G. Molnár, D. Upadhyay, M. Hopka, M. Van Nieuwstadt, and G. Orosz, "Exploiting V2X connectivity by delayed Lagrangian continuum traffic models," *Transportation Research Part C: Emerging Technologies*, 2020, under review.

[20] S. Feng, Y. Zhang, S. E. Li, Z. Cao, H. X. Liu, and L. Li, "String stability for vehicular platoon control: Definitions and analysis methods," *Annual Reviews in Control*, vol. 47, pp. 81–97, 2019.

[21] G. Orosz, R. E. Wilson, and G. Stépán, "Traffic jams: dynamics and control," *Philosophical Transactions of the Royal Society A: Mathematical, Physical and Engineering Sciences*, vol. 368, no. 1928, pp. 4455–4479, 2010.

[22] H. von Allwörden and I. Gasser, "On a general class of solutions for an optimal velocity model on an infinite lane," *Transportmetrica A: Transport Science*, pp. 1–20, 2020.

[23] S. S. Avedisov, G. Bansal, A. K. Kiss, and G. Orosz, "Experimental verification platform for connected vehicle networks," in *Proceedings of the 21st IEEE International Conference on Intelligent Transportation Systems*, Maui, HI, USA, 2018, pp. 818–823.

[24] A. Aw and M. Rascle, "Resurrection of "second order" models of traffic flow," *SIAM Journal on Applied Mathematics*, vol. 60, no. 3, pp. 916–938, 2000.

[25] H. M. Zhang, "A non-equilibrium traffic model devoid of gas-like behavior," *Transportation Research Part B: Methodological*, vol. 36, no. 3, pp. 275–290, 2002.

[26] L. Zhang and G. Orosz, "Motif-based design for connected vehicle systems in presence of heterogeneous connectivity structures and time delays," *IEEE Transactions on Intelligent Transportation Systems*, vol. 17, no. 6, pp. 1638–1651, 2016.

[27] V. Giammarino, M. Lv, S. Baldi, P. Frasca, and M. L. Delle Monache, "On a weaker notion of ring stability for mixed traffic with human-driven and autonomous vehicles," in *Proceedings of the 58th IEEE Conference on Decision and Control*, Nice, France, 2019, pp. 335–340.

[28] M. Krstic and A. Smyshlyaev, *Boundary control of PDEs: A course on backstepping designs*. Philadelphia: SIAM, 2008.

[29] H. Yu and M. Krstic, "Traffic congestion control for Aw-Rascle-Zhang model," *Automatica*, vol. 100, pp. 38–51, 2019.